Segmental and Local Chain Mobilities in Elastomers by $^{13}C-^{1}H$ Residual Heteronuclear Dipolar Couplings

Mingfei Wang, Marko Bertmer,* Dan E. Demco, and Bernhard Blümich

Institute of Technical Chemistry and Macromolecular Chemistry, Worringer Weg 1, 52056 Aachen, Germany

Received: April 13, 2004; In Final Form: May 19, 2004

Site-selective information about local segmental motions of individual CH_n fragments can be obtained by the determination of $^{13}C-^{1}H$ heteronuclear dipolar couplings. A systematical study was performed by measuring heteronuclear residual dipolar couplings of natural rubber samples with different cross-link densities using static and MAS solid-state NMR techniques such as SEDOR (spin-echo double resonance), REDOR (rotational-echo double resonance) and heteronuclear double-quantum (HeDQ) buildup curves. Even under static conditions, all five CH_n fragments of the monomer unit can be separated. $^{13}C-^{1}H$ residual dipolar couplings and scaled average order parameters extracted from the different experiments show a linear correlation with the cross-link density. However, the residual dipolar couplings are also dependent on the individual functional group. In other words, the local rotational motions of the functional groups are superimposed on the segmental motions of the chain segment and have to be taken into account in the prediction of the dynamic order parameter. From our analysis, the REDOR experiment gives the most reliable results and shows the largest dependence on the cross-link density. Because of the small residual dipolar couplings, the heteronuclear *J*-coupling cannot be neglected in the analysis of the experimental data. The described methods can also offer site-selective information for soft solids with even larger values of the cross-link density than those investigated in this study.

1. Introduction

Cross-linked elastomers are materials with high technological importance and widespread application.[1,2] The characterization of these materials including the correlation of macroscopic (viscoelastic) properties like mechanical stress with information about the microscopic structure is therefore of great scientific and technological interest. This can lead to a better understanding of material properties and consecutively the development of improved materials. In this context, the determination of cross-link densities as a major factor for the stiffness and strength of elastomers is one of the central goals. Swelling experiments are commonly used to estimate the cross-link density by comparing the weight at equilibrium swelling in a good solvent to that of the dry elastomer. Nuclear magnetic resonance (NMR)—especially in the solid-state—has been intensively applied to the study of cross-linked elastomers for the characterization of the chemistry of cross-links[3,4] as well as for the determination of chain dynamics and segmental mobility.[5−13] Mainly proton transverse magnetization relaxation measurements are widely applied to study cross-linking in elastomers[5,6,8,14,15] even in inhomogeneous magnetic fields.[16,17] The overall response of the spin system is often interpreted in terms of a residual second moment (M_2) in transverse relaxation measurements.[6,8] A different strategy makes use of Hahn echo, stimulated echo, and mixed echo experiments to determine residual second moments using the dipolar correlation effect (DCE) method.[9,11,12] ^{1}H multiple quantum experiments are among those techniques that reveal more localized information in natural rubber[13] and poly(dimethylsiloxane).[18] The determination of quadrupolar couplings in isotopically labeled elastomers by studying the ^{2}H nucleus has also been very effective, although accurate and exact labeling can be quite complicated.[19] Experiments involving the ^{13}C nucleus were made by studying the $^{1}H-^{13}C$ cross-polarization rates[6] and measurements of the proton rotating-frame relaxation time $T_{1\rho}$[20] as well as a separation of proton line widths according to ^{13}C chemical shifts with a 2D WISE experiment.[7] Residual proton dipolar couplings were derived and the results correlated with the cross-link density.

Quantifications of the experiments mentioned above, however, are quite complicated and often depend strongly on the polymer model used. On the other hand, residual dipolar couplings resulting from topological constraints and therefore anisotropic chain motions are directly sensitive to the dynamics in elastomer systems. The generally strong dipolar coupling is reduced to a much smaller value by fluctuations of the polymer chains, the degree of attenuation of these couplings being influenced by the cross-link density. Therefore, residual dipolar couplings are a direct indicator of the motions present in a polymer or elastomer. Attempts to measure residual dipolar couplings quantitatively were mainly done by observing the proton spin system.[13,21,22] A review of different one- and two-dimensional NMR techniques for the determination of residual dipolar couplings can be found in the literature.[23]

In this paper, we report the evaluation of heteronuclear residual dipolar couplings between ^{13}C and ^{1}H in a series of natural rubber samples with different cross-link densities. Reasons for choosing the heteronuclear couplings is on one hand the larger chemical shift dispersion of carbon compared to protons that allows for a selective detection of residual dipolar couplings of individual functional groups, i.e., CH_n fragments. All five functional groups of the monomer unit can be resolved even for nonrotating samples. Furthermore, because of the direct bond between carbon and proton (excluding quaternary carbons),

* Corresponding author. E-mail: mbertmer@mc.rwth-aachen.de.

10.1021/jp048392+ CCC: $27.50
Published on Web 06/25/2004

the heteronuclear residual dipolar coupling is much less influenced by the coupling of remote protons as opposed to the homonuclear residual dipolar couplings among protons. Therefore, localized information for each functional group can be extracted similar to ^{2}H measurements. The information content of local ^{13}C−^{1}H heteronuclear dipolar couplings was demonstrated in rigid organic solids using a two-dimensional cross-polarization experiment.[24] It was shown that the main contribution to the ^{1}H spinning sideband pattern comes from the heteronuclear dipolar coupling.

Motion in lipid bilayers also reduces heteronuclear dipolar couplings similar to elastomers. For this system, Gross et al.[25] developed a method to determine residual ^{13}C−^{1}H couplings in a two-dimensional MAS NMR experiment (DROSS). In solution NMR, partial alignment of large molecules—predominantly proteins—also leads to a residual dipolar coupling since the molecular motion is slightly restricted in appropriate solvents and concentrations. In this case, residual dipolar couplings can help in obtaining additional structural information[26−28] that is not available in dilute solutions and is of great importance for the determination of the 3D structure of proteins or enzymes. However, it should be noted that in solution the residual dipolar coupling is only a small contribution to the (isotropic) *J*-coupling whereas in the solid-state we consider the down scaling of the strong dipolar coupling from about 20 or 30 kHz down to about 100 Hz. But in our case, the values for the heteronuclear dipolar and *J*-coupling are also of comparable size.

Different measurement techniques that were used successfully for the determination of heteronuclear dipolar couplings in rigid solids were investigated for their applicability to measure residual dipolar couplings in soft solids. Among those, the measurement of heteronuclear double quantum (HeDQ)[29−32] buildup curves and spin-echo double resonance (SEDOR)[33,34] as well as rotational-echo double resonance (REDOR)[32,35,36] experiments were selected. For the first time, SEDOR and REDOR techniques are applied to elastomers with highly mobile CH_n fragments. Originally, SEDOR and REDOR was developed to measure weak dipolar couplings, e.g., ^{13}C−^{15}N,[35,37] and in our case the ^{1}H−^{13}C coupling in elastomers is also greatly reduced by motion. For rigid solids, Fyfe et al.[38] compared the accuracy of distance measurements via heteronuclear dipolar couplings between cross-polarization, REDOR, and TEDOR (transferred-echo double resonance) experiments on silicates. Their conclusion is that these experiments give comparable results whereas the appropriate technique to choose depends on the different relaxation times (spin−lattice, spin−spin, spin−lattice in the rotating frame) of the sample. In our case, it is shown below that further adjustments have to be made by going from rigid solids to heterogeneous soft solids in the interpretation of the results obtained with the different measurement techniques, and the advantages and disadvantages of these techniques for the measurement of ^{13}C−^{1}H residual heteronuclear dipolar couplings are summarized.

2. Experimental Section

2.1. Samples. Samples of vulcanized natural rubber (predominantly *cis*-polyisoprene) with different content of sulfur were obtained from Dunlop AG, Hanau, Germany. The general composition is 100 phr (parts per hundred rubber) standard Malaysian rubber (SMR 10), 3 phr stearic acid, and 2 phr zinc oxide. The accelerator was benzothiazyl-2-*tert*-butylsulfenamide (TBBS). The vulcanization temperature was 160 °C for all samples. Sample notations, sulfur, and TBBS content as well as the vulcanization time are summarized in Table 1. The vulcanization time was determined by measuring the low-frequency shear modulus in a Monsanto MDR-2000-E vulcameter directly after vulcanization with a frequency of 1.67 Hz and an oscillation amplitude of ±0.5°. As the amounts of sulfur and accelerator are identical and incremented in the same way, it is valid to assume that the cross-link density correlates linearly with the sulfur content.

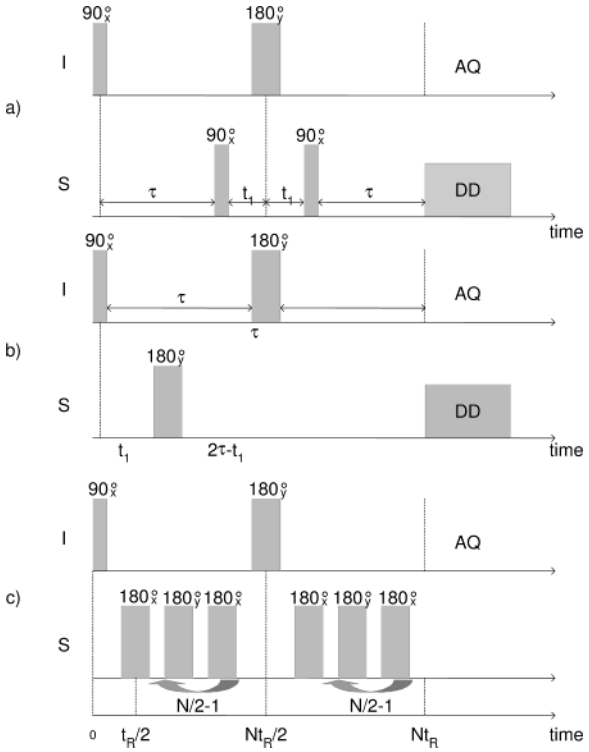

Figure 1. Pulse sequences employed in this investigation: (a) scheme for excitation of heteronuclear double quantum (HeDQ) coherences, where the delay t_1 is on the order of 2 μs for phase switching of the pulses; (b) SEDOR sequence with fixed echo time 2τ, where t_1 is incremented from 0 to τ; (c) REDOR sequence (t_R is the time for one rotor period; *N* indicates the number of rotor cycles). The reference experiment is performed by omitting the proton pulses. High-power heteronuclear ^{1}H decoupling is denoted by DD.

TABLE 1: Sample Composition and Vulcanization Parameters of Natural Rubber Samples NR1−NR5

sample	phr sulfur	phr TBBS	vulcanization time (min)
NR1	1	1	14
NR2	2	2	12
NR3	3	3	10.5
NR4	4	4	8
NR5	5	5	7

2.2. NMR Experiments. Solid-state NMR experiments were performed on a Bruker Avance DSX 500 NMR spectrometer with ^{1}H and ^{13}C frequencies of 500.46 and 125.84 MHz, respectively. For the HeDQ and SEDOR experiments, a Bruker 7 mm MAS probe was used under nonspinning conditions, whereas the REDOR experiments were performed with a Bruker 4 mm MAS probe at a spinning speed of 10 kHz. The different pulse sequences used are shown in Figure 1. 90° pulse lengths were 6 μs for the 7 mm probe and 5.5 μs for the 4 mm probe. Recycle delays of 5 s were sufficient to exceed $5T_1$ for all ^{13}C signals as determined by inversion−recovery (IR) measurements (data not shown). Direct excitation of the carbon nucleus is

preferable to cross-polarization from abundant protons in natural rubber because of the low cross-polarization efficiency due to the small heteronuclear residual dipolar couplings. Even under static conditions, all different ^{13}C sites are well resolved which enables a selective determination of the residual dipolar couplings for each CH_n fragment (see below).

For the HeDQ experiments (cf. Figure 1a), a spin-echo sequence was performed on the ^{13}C channel (I), with two 90° pulses on the ^{1}H channel (S) just before and after the 180° pulse on ^{13}C to excite $^{1}H-^{13}C$ double quantum coherences.[29] The delay t_1 is on the order of the 2 μs needed for phase switching of the pulses. The first ^{1}H pulse creates double quantum coherence, while the second one reconverts it to observable ^{13}C single quantum coherence, and the echo is detected. A suitable phase cycle was employed to select only signal that passed through a heteronuclear double quantum coherence. By incrementing the echo time so-called buildup curves are recorded. In general, the faster the buildup of DQ coherences, the larger is the dipolar coupling.

In the SEDOR experiment, a Hahn echo is used as well on the ^{13}C channel (cf. Figure 1b). But in this case, a 180° pulse on the ^{1}H channel prevents refocusing of the full echo for those carbons in close proximity to protons and an attenuated echo signal is detected. Two variations of the SEDOR technique exist to record a full curve, either incrementing the echo time with application of the 180° pulses on both channels at the same time[33] or alternatively with a fixed echo time and variation of the position of the proton 180° pulse during the first half of the echo.[34] In both cases, reference measurements are performed without the 180° pulse on the proton channel. We employed the latter method with an echo time of 2 ms that is selected so that there is still enough signal intensity and already significant signal attenuation by the proton pulse. Additionally, in this pulse sequence only one reference experiment has to be performed. For each delay t_1, the difference between the dephasing (S) and the reference spectra (S_0)—normalized to the reference spectra—is calculated and graphically represented as a function of the evolution time. Clearly, the faster the rise of this curve, the larger is the heteronuclear coupling.

Finally, several variations of the REDOR sequence, which is the analogue of SEDOR under MAS, exist,[32,35,39] mainly differing in the distribution of the two 180° pulses per rotor period on the two channels. For rigid C−H systems, it was described to be advantageous to have only minimal differences in the pulse scheme on the proton channel between dephasing and nondephasing experiments so that the influence of homonuclear $^{1}H-^{1}H$ couplings is minimized.[32] However, we tested the different variants and found no significant differences among them which is probably due to the much smaller homonuclear dipolar couplings in natural rubber. The reference experiment of the sequence shown in Figure 1c is performed by omitting the proton pulses. To minimize resonance offset effects and effects from pulse imperfections, for the dephasing pulses the XY-8 scheme was employed.[40]

3. Theory

Whereas in rigid systems the dipolar coupling is much larger than the scalar or *J*-coupling, this is not necessarily the case in mobile systems like natural rubber. In opposition to the homonuclear $^{1}H-^{1}H$ case, where $^{2}J_{HH}$-couplings are relatively small, $^{1}J_{CH}$-couplings are appreciably large and can be determined in a ^{13}C spectrum under spinning conditions without proton decoupling (see below).

3.1. Residual Dipolar Coupling. The heteronuclear scalar and dipolar Hamiltonian can be written for a spin-pair in the absence of motion as

$$\mathscr{H} = 2(\pi J_{IS} + \omega_D)\hat{I}_z\hat{S}_z \tag{1}$$

with

$$\omega_D = D_{IS}\frac{1}{2}(3\cos^2\theta_{IS} - 1) \tag{2}$$

and

$$D_{IS} = \frac{\mu_0}{4\pi}\frac{\gamma_I\gamma_S\hbar}{r_{IS}^3} \tag{3}$$

D_{IS} is the rigid dipolar coupling between—in this case—a ^{13}C and a ^{1}H spin. θ_{IS} is the angle between the internuclear vector and the static magnetic field, and the distance between both nuclei is denoted by r_{IS}.

Motions in polymeric melts or in our case natural rubber at room temperature reduce the static dipolar coupling to a residual dipolar coupling.[41] The coupling is not reduced to zero since these motions are anisotropic due to the presence of topological constraints created by chemical cross-links as well as physical entanglements. To describe the effect of motions on the angular dependence of the dipolar couplings we make use of the scale-invariant model that assumes that dipolar interactions are averaged over all conformations of the chain with the constraint that the end-to-end vector is fixed.[8,13,27] This model was successfully adapted to the determination of proton−proton residual dipolar couplings, and we also adapt it for the elucidation of heteronuclear residual dipolar couplings. Applying this model, we relate the C−H internuclear vector as well as the static magnetic field to this end-to-end vector as a new reference frame which leads to

$$\langle\mathscr{H}\rangle = 2\left(\pi J_{IS} + \langle\omega_D\rangle\frac{1}{2}(3\cos^2\beta - 1)\right)\hat{I}_z\hat{S}_z \tag{4}$$

where

$$\langle\omega_D\rangle = D_{IS}\frac{k}{N_k^2 a^2}\vec{R}^2 S_{CH} \tag{5}$$

is the residual dipolar coupling with $S_{CH} = {}^1/_2\langle 3\cos^2\zeta_{IS}(t) - 1\rangle$ being the average order parameter which is identical to the largest component S_{zz} of the Saupe order tensor.[27] $\vec{R}$ is the end-to-end vector of the polymer chain. ζ denotes the polar angle between the internuclear vector $\vec{r}_{IS}$ and $\vec{R}$, and β is the polar angle between the static magnetic field $\vec{B}_0$ and $\vec{R}$. $\langle\cdots\rangle$ represents the average over the molecular reorientation. As we assume a rigid body approach for the backbone chain (the end-to-end vector), no time average for the β-term is needed. The parameters N_k, k, and a are deduced from the assumption that the intercross-link chain consists of N_k statistical segments (Kuhn segments) of length a,[5,41] which are not to be confused with the number of repeat units and its length but are proportional to it. k is a geometrical factor that depends on the model for the chain statistics. As an example, for a chain of freely jointed segments $k = {}^3/_5$.[42]

For the orientation of the end-to-end vector in a disordered polymer it is quite valid to assume a Gaussian distribution of the end-to-end vector[41] which results in $\langle R^2\rangle \approx N_k a^2$.[5] We combine N_k and k into $N_{eff} = N_k/k$ as an effective number of the statistical segments. Therefore, the residual dipolar coupling

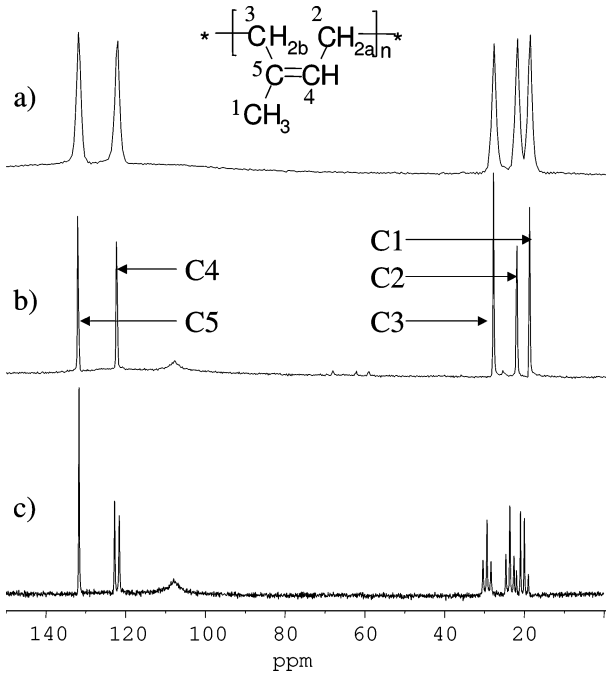

Figure 2. ^{13}C Bloch decay spectra of sample NR5. The assignments of the signals is given in the inset. Key: (a) static spectrum with ^{1}H decoupling; (b) 5 kHz MAS spectrum with ^{1}H decoupling; (c) 5 kHz MAS spectrum without ^{1}H decoupling showing the heteronuclear *J*-couplings. The small signal at 117 ppm in parts b and c is due to the ^{13}C background signal of the probe.

scales with $1/N_{\mathrm{eff}}$ or $1/N_k$. It is this dependence that we want to stress with our experiments. In the following we include N_{eff} into the order parameter to obtain a scaled dynamic order parameter $S_{\mathrm{CH}}^{\mathrm{sc}} = S_{\mathrm{CH}}/N_{\mathrm{eff}}$.

Vulcanized natural rubber is a heterogeneous material. Because of the random sulfur cross-linking, a distribution of the number of monomer units between cross-link points exists. Additionally, physical entanglements and chain ends are present that complicate the analysis. Because of this, depending on the position in the polymer chain, different residual heteronuclear couplings exist, so that only average residual couplings can be determined. In previous models for the analysis of ^{1}H transverse relaxation times as well as ^{1}H$-^{1}$H homonuclear residual dipolar couplings, isolated proton spin pairs were assumed to exist along the polymer chain with all spin pairs having identical residual dipolar couplings.[5] This approach is certainly an oversimplification as was also discussed in a ^{2}H investigation of natural rubber.[19] As all different CH_n fragments can be separated in the ^{13}C spectrum of natural rubber, the evaluation of their residual dipolar couplings has to be treated individually. For the CH fragment, the above description for a spin-pair can be applied directly. As the quaternary carbon is not directly bound to a proton, the determination of an average order parameter is of limited value, and we exclude the quaternary carbon signals from quantification. For the methylene and methyl carbons, the interaction of two or three protons at the same distance and their relative orientations to the carbon have to be taken into account. It was shown in solution NMR[26] that in the evaluation of residual heteronuclear couplings for methylene and methyl carbons one obtains the sum of the individual C$-$H pair couplings.

3.2. Data Analysis. Residual dipolar couplings are obtained from the HeDQ buildup curves by full simulation including the heteronuclear *J*-couplings determined by a ^{13}C-MAS spectrum without ^{1}H-decoupling (see Figure 2c). In general a parabolic fit to the initial part of the buildup curve can also be done to determine the residual dipolar coupling. However, calibration of DQ buildup curves using a reference sample with known dipolar coupling is necessary which was not done in this case. Therefore, buildup curves using a Gaussian distribution of dipolar couplings were calculated using the SIMPSON program[43] combined with an algorithm using Mathematica.[44] For the methylene and methyl groups the geometric positions of the protons were taken into account. The simulated buildup curves were then combined with an exponential decay function to account for the relaxation of the single quantum coherences. Details of the simulation procedure can be found elsewhere.[45] The mean values of the distribution functions used for the simulation are listed in Table 2. From these, the average order parameters were calculated according to eq 5 by taking the rigid C$-$H couplings to be 22.7 kHz.[46] We note, however, that the full buildup curve contains a mixture of different effects, i.e., the effect of remote spins and cross-relaxation of different coherences. The initial part of the buildup curve would be superior to use, although it is necessary to calibrate the signal intensity which could be done by comparison with a sample with known dipolar coupling[47] or as recently presented by a calibration of double quantum, zero-quantum, and longitudinal magnetization experiments.[18] Nevertheless, simulation of the full buildup curve was successfully employed before and is also a valid approach.[45,48,49]

TABLE 2: Residual Dipolar Couplings and Average Order Parameters Determined with HeDQ, SEDOR, and REDOR Measurements for the Individual CH_n Fragments of the Sample Series[a]

		HeDQ		SEDOR		REDOR	
fragment	sample	$\langle\omega_{\mathrm{D}}\rangle$	$S_{\mathrm{CH}}^{\mathrm{sc}}$	$\langle\omega_{\mathrm{D}}\rangle$	$S_{\mathrm{CH}}^{\mathrm{sc}}$	$\langle\omega_{\mathrm{D}}\rangle$	$S_{\mathrm{CH}}^{\mathrm{sc}}$
CH	NR1	160	0.007	69	0.003	53	0.002
	NR2	180	0.008	84	0.003	109	0.005
	NR3	220	0.010	169	0.007	147	0.006
	NR4	220	0.010	201	0.009	179	0.008
	NR5	280	0.012	220	0.010	208	0.009
CH_{2a}	NR1	160	0.007	165	0.007	91	0.004
	NR2	200	0.009	204	0.009	178	0.008
	NR3	200	0.009	250	0.011	208	0.009
	NR4	200	0.009	291	0.013	224	0.010
	NR5	260	0.012	262	0.012	253	0.011
CH_{2b}	NR1	160	0.007	147	0.006	74	0.003
	NR2	180	0.008	147	0.006	106	0.005
	NR3	220	0.010	195	0.009	138	0.006
	NR4	220	0.010	230	0.010	173	0.008
	NR5	260	0.011	279	0.012	199	0.009
CH_3	NR1	80	0.004	35	0.002	59	0.003
	NR2	100	0.004	54	0.002	72	0.003
	NR3	140	0.006	113	0.005	116	0.005
	NR4	140	0.006	151	0.007	121	0.005
	NR5	180	0.008	137	0.006	164	0.007

[a] Values are for one C$-$H coupling for each CH_n fragment. Uncertainties are about 10% for the HeDQ measurements and 5% for both SEDOR and REDOR measurements.

For the SEDOR and REDOR experiments, the analysis is simpler because the initial slope is directly related to the square of the dipolar coupling (and the *J*-coupling) which results from a Taylor series expansion of the analytical formulas for the SEDOR and REDOR experiments.[34,50,37] Following eq 5 and assuming Gaussian statistics the average over the distribution of the end-to-end vector $\langle(R^2/N_k a^2)^2\rangle = {}^1/_3$,[13,49] one obtains

$$\text{SEDOR:}\quad \frac{\Delta S}{S_0} = \frac{S_0 - S}{S_0} = \left\{ {J_{\mathrm{IS}}}^2 + \frac{4}{15}(D_{\mathrm{IS}} S_{\mathrm{CH}}^{\mathrm{sc}})^2 \right\} 2\pi^2\tau^2 \qquad (6)$$

$$\text{REDOR:}\quad \frac{\Delta S}{S_0} = \frac{S_0 - S}{S_0} = \frac{16}{45}(D_{\mathrm{IS}} S_{\mathrm{CH}}^{\mathrm{sc}})^2 N^2 {t_{\mathrm{R}}}^2 \qquad (7)$$

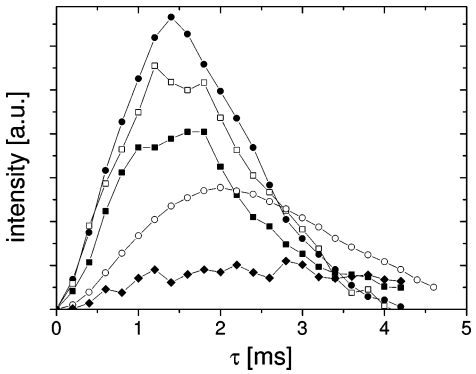

Figure 3. HeDQ buildup curves for sample NR1 illustrating the differences between the individual CH_n fragments. The solid lines are guides for the eye. Identification of curves: CH_3 (solid squares); CH_{2a} (solid circles); CH_{2b} (open squares); CH (open circles); quaternary carbon (solid diamonds).

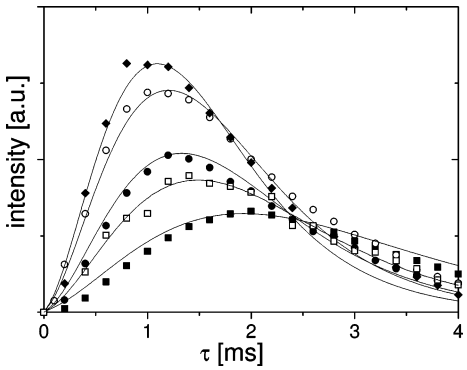

Figure 4. HeDQ buildup curves of the CH fragment for samples NR1−NR5. The solid lines represent fits using the procedure described in the text. Identification of the curves: NR1 (solid squares); NR2 (open squares); NR3 (solid circles); NR4 (open circles); NR5 (solid diamonds).

Here τ represents half of the echo time in the SEDOR experiment, in the REDOR experiment t_R represents the time for one rotor period and N_C the number of rotor cycles (see Figures 1b and c). Using eqs 6 and 7, residual dipolar couplings and with that the average order parameter can be easily obtained by a parabolic fit of the initial part of the SEDOR and REDOR curves, respectively. The parabolic fit is reasonably valid up to a difference signal of 20%.[37] As can be seen, in the REDOR sequence, the *J*-coupling does not affect the difference signal, therefore the parabolic fit directly results in the residual dipolar coupling.

For the methylene and methyl groups the fit functions have to be modified. It can be shown that the initial part of the SEDOR and REDOR difference curves is simply dependent on the sum of two or three dipolar couplings for the methylene and methyl signals, respectively,[51] without the need to incorporate the relative positions of the spins:

$$\text{SEDOR: } CH_2 \quad \frac{\Delta S}{S_0} = 4\pi^2\tau^2\left\{J_{IS}{}^2 + \frac{4}{15}(D_{IS}S^{sc}_{CH_2})^2\right\} \tag{8}$$

$$CH_3 \quad \frac{\Delta S}{S_0} = 6\pi^2\tau^2\left\{J_{IS}{}^2 + \frac{4}{15}(D_{IS}S^{sc}_{CH_3})^2\right\} \tag{9}$$

$$\text{REDOR: } CH_2 \quad \frac{\Delta S}{S_0} = \frac{32}{45}(D_{IS}S^{sc}_{CH_2})^2N^2t_R{}^2 \tag{10}$$

$$CH_3 \quad \frac{\Delta S}{S_0} = \frac{48}{45}(D_{IS}S^{sc}_{CH_3})^2N^2t_R{}^2 \tag{11}$$

4. Results and Discussion

In the following, the experimental results of the different measurement techniques are described and analyzed, followed by a comparison between the different techniques and their results. Figure 2 depicts the static (a) and 5 kHz MAS (b) ^{13}C Bloch-decay spectra of sample NR5 with ^1H decoupling showing the resolution of the five CH_n fragments even under static conditions together with the assignment of the individual signals seen by the enumeration of ^{13}C atoms in the monomeric unit shown in the inset. Without ^1H decoupling under MAS (Figure 2c) the $^1J_{CH}$-couplings can be resolved. The extracted values are 150 Hz for the CH group and 125 Hz for both CH_2 groups and the CH_3 group. *J*-couplings are identical for the individual CH_n fragments for all samples.

4.1. Heteronuclear Double Quantum (HeDQ) Experiments. To demonstrate the differences between the buildup behavior of the individual CH_n fragments, Figure 3 shows the HeDQ buildup curves for sample NR1. The much slower buildup for the quaternary carbon is clearly visible. This can be seen in all experiments and demonstrates that couplings are due to intramolecular and not intermolecular interactions which was discussed contradictory in the literature.[52,53] Buildup curves for the CH fragment with different amounts of sulfur are summarized in Figure 4. Qualitatively the excitation time for maximum DQ efficiency shifts to longer times with decreasing amounts of sulfur in the samples, and with that decreasing cross-link density indicating smaller couplings. However, differences between samples NR3 and NR4 are smaller than between NR4 and NR5.

A full simulation of the buildup curves results in the residual C−H dipolar couplings, and average order parameters calculated from that, both are summarized in Table 2. To demonstrate the quality of the fit, the simulated curves are included for the five samples in Figure 4. Plots of the residual dipolar couplings vs the sulfur content in Figure 5, parts a−d reveal reasonably good linear correlations indicating the usefulness of this method to determine cross-link densities. We note, however, that NR3 and NR4 give almost identical fit values and the accuracy of the coupling is ±20 Hz because of the fitting procedure and the signal-to-noise ratio. A linear extrapolation of the data reveals that even at 0 phr sulfur (no chemical cross-linking) the residual dipolar coupling is different from zero, which is attributed to topological constraints of the chains that prevent an isotropic motion.

4.2. SEDOR Experiments. Results for the SEDOR experiments obtained with the pulse sequence version of Figure 1b are depicted in Figures 6 and 7 for the CH_n fragments of sample NR4 and for the CH fragment of the different samples, respectively. Similar observations as for the HeDQ experiments are made, that is, the much slower signal buildup of the quaternary carbons and the increase of signal buildup with increasing sulfur content. The initial slope up to a difference signal of 20% of each curve was analyzed by fits of eqs 6, 8, and 9 from which the residual dipolar couplings and order parameters were extracted. The values determined are also included in Table 2 and plotted in Figure 5, parts a−d. The residual dipolar coupling increases linearly with increasing amount of sulfur. However, especially for the CH and CH_3 group, smaller absolute values for the residual dipolar couplings are obtained compared to those derived from the HeDQ data. An explanation for this is given below.

4.3. REDOR Experiments. Figures 8 and 9 display the results of the REDOR experiments for sample NR4 and the CH fragment of the different samples, respectively. The experiments

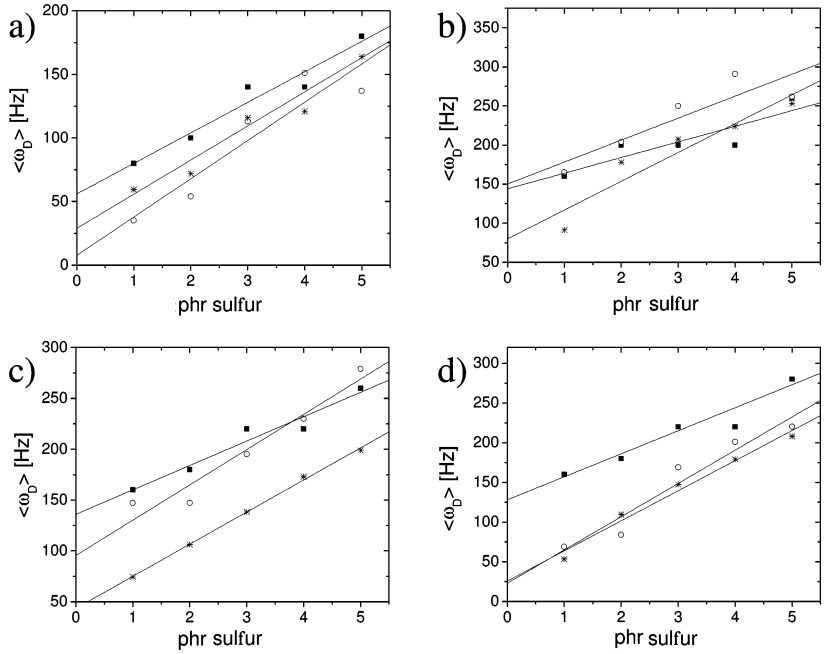

Figure 5. Extracted residual dipolar couplings as a function of the amount of sulfur in samples NR1−NR5. The linear correlation is indicated by solid lines. Key: (a) CH_3; (b) CH_{2a}; (c) CH_{2b}; (d) CH. Identification: HeDQ (solid squares); SEDOR (open circles); REDOR (stars).

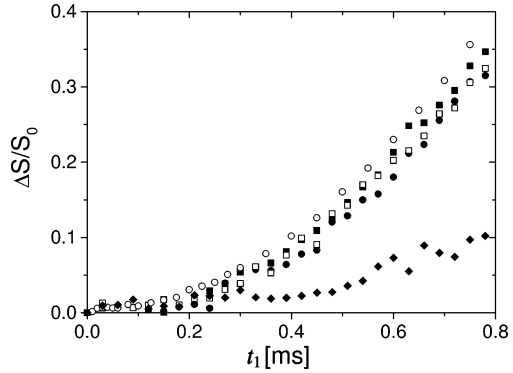

Figure 6. SEDOR curves for sample NR4. Labeling of curves as in Figure 3.

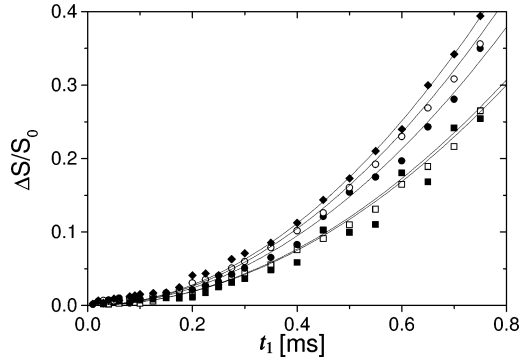

Figure 7. SEDOR curves of the CH fragment. Indication of samples: NR1 (solid squares); NR2 (open squares); NR3 (solid circles); NR4 (open circles); NR5 (solid diamonds). The lines represent fits to eq 6.

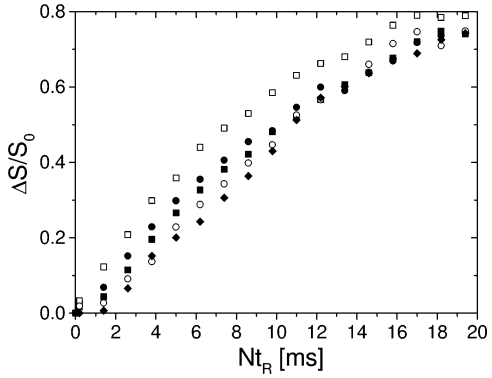

Figure 8. REDOR curves for sample NR4. The curves are labeled as in Figure 3.

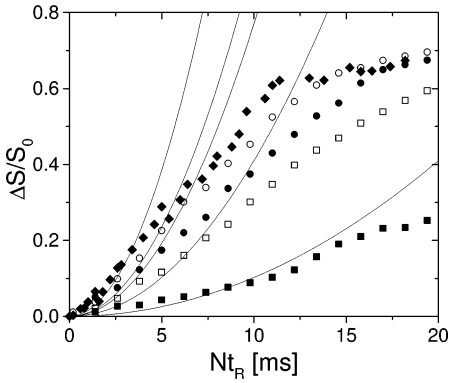

Figure 9. REDOR curves of the CH fragment. Identification of the curves: NR1 (solid squares); NR2 (open squares); NR3 (solid circles); NR4 (open circles); NR5 (solid diamonds). The lines represent fits of eq 7.

were performed at a spinning speed of 10 kHz with the pulse sequence of Figure 1c. As mentioned above, no differences were detected with different versions of the REDOR sequence, so that the influence of homonuclear dipolar couplings should be negligible. The residual dipolar couplings were analyzed by a parabolic fit of the initial part of the curves up to a difference signal of 20% using eqs 7, 10, and 11. The results are also included in Table 2 and displayed in Figure 5, parts a−d. It can be seen that the linear correlation with the sulfur content is very good. In general, the dipolar couplings determined by the REDOR experiments are somewhat smaller than those measured in the SEDOR and HeDQ experiments. The reason for this is given in the next section.

4.4. Comparison of NMR Methods. A comparison of residual dipolar couplings obtained by the three different NMR techniques shows a linear correlation in all cases with the amount of sulfur in the natural rubber samples but shows differences in the absolute couplings and the determined order parameters. The slopes of the linear correlation function of the dipolar couplings with the sulfur content are comparable, those for the REDOR experiments being a little larger which also means that REDOR is more sensitive to changes in the dipolar couplings. This is probably due to the fact that REDOR—as opposed to SEDOR and HeDQ—is unaffected by the isotropic heteronuclear *J*-coupling. The highest values for the dipolar couplings were obtained for the HeDQ experiments and the lowest for the REDOR experiments. This demonstrates the general applicability of these techniques to characterize cross-link densities in a sample series. However, to explain the different absolute values between the measurement techniques one has to take into account the nature of the dipolar network edited by the different NMR techniques.

As noted above, due to a distribution of residual dipolar couplings one can only obtain an average residual coupling. HeDQ experiments of heterogeneous materials emphasize larger couplings because they lead to a faster buildup of multiple quantum coherence. Furthermore, the HeDQ experiment is an absolute measurement technique in contrast to SEDOR and REDOR where the difference curve accounts for the signal response of all carbons with the same weighting because of the referencing. The presence of homonuclear $^1H-^1H$ couplings also affects the HeDQ buildup curves in a way that leads to faster signal buildup pretending a larger heteronuclear residual dipolar coupling. Therefore, the HeDQ experiments result in larger residual dipolar couplings than those derived from SEDOR and REDOR experiments, but it is clear that in the natural rubber system studied here the differences are small.

The SEDOR experiment for the CH_{2a} groups reveals a slope smaller than those measured by all other experiments. The reason for this could be that in the static experiments the separation of the CH_{2a} and CH_3 groups is incomplete so that small errors are included in the analysis of the signal intensities.

Overall, the REDOR experiments result in the smallest couplings compared to those of the SEDOR and HeDQ experiments. This can be explained as the result of sample spinning which removes or at least reduces the homonuclear as well as the heteronuclear dipolar couplings. While the heteronuclear coupling is reintroduced through the pulse sequence, the homonuclear couplings between protons are scaled because of sample spinning. In rigid systems, the removal of $^1H-^1H$ homonuclear couplings was explained to take place just at spinning speeds above 20 kHz,[32] but as in our case we deal with small residual couplings, this effect is assumed to take place already at spinning speeds of 10 kHz and even below. An indication for this can also be taken from the fact that high-resolution ^1H spectra can already be seen at spinning speeds below 2 kHz and the line width does not change with increasing spinning speed. REDOR experiments therefore yield "pure" heteronuclear couplings. In the SEDOR experiment, homonuclear $^1H-^1H$ couplings affect the behavior of the difference curve mainly at longer echo times. There is only a minor effect on the initial part of the curve that was used in the analysis above. One can therefore conclude that the existence of homonuclear couplings only has a minor effect on the error in determining heteronuclear dipolar couplings. We expect that the different residual dipolar couplings in SEDOR and REDOR experiments are therefore due to remote heteronuclear couplings between a carbon and protons of another CH_n fragment resulting in larger heteronuclear couplings in the SEDOR experiments. Sample spinning reduces the "effective" spin-system to protons bound directly to the carbon spin and results in more accurate values.

Comparing the individual functional groups, the methylene groups show the largest values with those of the CH_{2a} fragment being the largest of all. Values for the CH fragment are comparable and slightly smaller. As expected, for the methyl group the smallest values are obtained because of the additional rotation around the C_3 axis. These results indicate different mobilities for the different CH_n fragments. This is due to the superposition of the segmental motion, which is responsible for the linear dependence of the residual coupling with the cross-link density, and the local rotational motion of each functional group. This information has never been discovered before and is only accessible because of the spectral resolution on the ^{13}C nucleus even under nonspinning conditions. While the elucidation of homonuclear residual dipolar couplings only enabled the determination of the segmental motion and the local motions of the functional groups as a whole this piece of information is new. This clearly demonstrates the advantage of our approach to investigate heteronuclear residual dipolar couplings.

5. Conclusions

For the first time, we described the application of different techniques for the elucidation of $^{13}C-^1H$ heteronuclear residual dipolar couplings on a series of natural rubber samples with different amounts of sulfur. Heteronuclear double quantum (HeDQ) and spin-echo double resonance (SEDOR) as well as rotational-echo double resonance (REDOR) experiments all show a linear correlation between the residual dipolar coupling, following also the average order parameter, and the cross-link density. However, care has to be taken in obtaining exact absolute values not obscured by other effects. Two factors could be identified here: SEDOR and REDOR—opposed to HeDQ measurements—are difference measurements so that a relative dephasing of all ^{13}C nuclei is observed whereas in HeDQ measurements those with larger residual dipolar couplings are emphasized. In the case of natural rubber as a heterogeneous material having a distribution of couplings this effect is present although not very strong. Second, homonuclear $^1H-^1H$ couplings as well as the influence of remote heteronuclear $^1H-^{13}C$ couplings lead to an overestimation of the values extracted from the HeDQ and SEDOR data. Magic angle spinning (MAS) removes the effect of remote couplings to the difference signal leading to smaller values of the residual dipolar couplings in REDOR data compared to those extracted from SEDOR data. Homonuclear $^1H-^1H$ couplings influence the HeDQ experiment pretending higher heteronuclear couplings. This effect is smaller in SEDOR experiments and not present in REDOR experiments due to fast magic angle spinning. The sensitivity of residual dipolar couplings to changes in the cross-link density is larger for the REDOR experiments because the dephasing signal is only influenced by the dipolar couplings whereas in the static SEDOR and HeDQ experiments also the isotropic heteronuclear *J*-coupling affects the difference signal and the buildup curves, respectively. Furthermore, differences between the heteronuclear residual dipolar couplings of the individual functional groups indicate that two types of motions are responsible for the determined couplings. On one hand, the segmental mobility is present which is reflected by the linear correlation of the couplings with the cross-link density. But on the other hand, local rotational motions of the functional groups lead to

differences in the overall residual dipolar couplings. This information was obtained for the first time with this study.

Summarizing, all experiments could be used as a tool for process and quality control within a sample series. Especially, HeDQ and SEDOR experiments require no sample spinning and therefore can be run with rather simple equipment and possible effects due to heating or centrifugal forces by fast magic-angle spinning can be avoided. However, the HeDQ experiment suffers from lower signal intensity and SEDOR is preferable since its results are closer to those of the REDOR experiments showing effects of the directly bonded protons only and no influence of homonuclear couplings. The values of the residual dipolar couplings obtained from REDOR experiments are slightly lower, and REDOR is more sensitive to changes in the cross-link density. For accurate quantitative values we assume the REDOR experiment to describe the residual dipolar couplings of individual CH_n fragments best. In the static experiments, however, the isotropic *J*-coupling cannot be neglected in the data analysis.

Our results show that the site-selective residual dipolar couplings depend not only on the segmental motions but also on local isomerization transitions. Therefore, a more detailed insight into the network behavior at different length and time scales can be obtained.

Residual heteronuclear dipolar couplings in natural rubber can be obtained without the need for a model describing the molecular motions as in experiments where, e.g., dipolar correlation functions are evaluated. HeDQ, SEDOR, and REDOR experiments can also be applied for extracting this information to the whole class of soft solids and in samples with cross-link densities even higher than those studied here.

References and Notes

(1) Brydson, J. A. *Rubber Chemistry*; Applied Science: London, 1996.
(2) Mark, J. A.; Erman, B. *Elastomeric Polymer Network*; Prentice-Hall: Englewood Cliffs, NJ, 1992.
(3) Parker, D. D.; Koenig, J. L. *J. Appl. Polym. Sci.* **1998**, *70*, 1371−1383.
(4) Mori, M.; Koenig, J. L. *J. Appl. Polym. Sci.* **1998**, *70*, 1391−1399.
(5) Sotta, P.; Fülber, C.; Demco, D. E.; Blümich, B.; Spiess, H. W. *Macromolecules* **1996**, *29*, 6222−6230.
(6) Fülber, C.; Demco, D. E.; Weintraub, O.; Blümich, B. *Macromol. Chem. Phys.* **1996**, *197*, 581−593.
(7) Malveau, C.; Tekely, P.; Canet, D. *Solid State Nucl. Magn. Reson.* **1997**, *7*, 271−280.
(8) Brereton, M. G. *Macromolecules* **1990**, *23*, 1119−1131.
(9) Fechete, R.; Demco, D. E.; Blümich, B. *J. Chem. Phys.* **2003**, *118*, 2411−2421.
(10) Demco, D. E.; Hafner, S.; Fülber, C.; Graf, R.; Spiess, H. W. *J. Chem. Phys.* **1996**, *105*, 11285−11296.
(11) Ball, R. C.; Callaghan, P. T.; Samulski, E. T. *J. Chem. Phys.* **1997**, *106*, 7352−7361.
(12) Grinberg, F.; Garbarczyk, M.; Kuhn, W. *J. Chem. Phys.* **1999**, *111*, 11222−11231.
(13) Schneider, M.; Gasper, L.; Demco, D. E.; Blümich, B. *J. Chem. Phys.* **1999**, *111*, 402−415.
(14) Brereton, M. G. *Macromolecules* **1993**, *26*, 1152−1157.
(15) Menge, H.; Hotopf, S.; Heuert, U.; Schneider, H. *Polymer* **2000**, *41*, 3019−3027.
(16) Zimmer, G.; Guthausen, A.; Blümich, B. *Solid State Nucl. Magn. Reson.* **1998**, *12*, 183−190.
(17) Blümich, B.; Bruder, M. *Kautschuk Gummi Kunstst.* **2003**, *56*, 90−94.
(18) Saalwächter, K.; Ziegler, P.; Spyckerelle, O.; Haidar, B.; Vidal, A.; Sommer, J.-U. *J. Chem. Phys.* **2003**, *119*, 3468−3482.
(19) Gronski, W.; Stadler, R.; Jacobi, M. M. *Macromol.* **1984**, *17*, 741−748.
(20) Chaumette, H.; Grandclaude, D.; Tekely, P.; Canet, D.; Cardinet, C.; Verschave, A. *J. Phys. Chem. A* **2001**, *105*, 8850−9956.
(21) Callaghan, P. T.; Samulski, E. T. *Macromolecules* **1997**, *30*, 113−122.
(22) Eulry, V.; Tekely, P.; Humbert, F.; Canet, D.; Marcilloux, J. *Polymer* **2000**, *41*, 3405−3410.
(23) Demco, D. E.; Hafner, S.; Spiess, H. W. In *Spectroscopy of Rubbers and Rubbery Materials*; Litvinov, V. M., De, P. P., Eds.; Rapra Technology Ltd.: Shrewsbury, U.K., 2002.
(24) Palmas, P.; Tekely, P.; Canet, D. *Solid State Nucl. Magn. Reson.* **1995**, *4*, 105−111.
(25) Gross, J. D.; Warschawski, D. E.; Griffin, R. G. *J. Am. Chem. Soc.* **1997**, *119*, 796−802.
(26) Ottinger, M.; Delaglio, F.; Marquardt, J. L.; Tjandra, N.; Bax, A. *J. Magn. Reson.* **1998**, *134*, 365−369.
(27) Prestegaard, J. H.; Al-Hashimi, H. M.; Tolman, J. R. *Q. Rev. Biophys.* **2000**, *33*, 371−424.
(28) Brunner, E. *Concepts Magn. Reson.* **2001**, *13*, 238−259.
(29) Sakellariou, D.; Lesage, A.; Emsley, L. *J. Magn. Reson.* **2001**, *151*, 40−47.
(30) Sommer, W.; Gottwald, J.; Demco, D. E.; Spiess, H. W. *J. Magn. Reson. A* **1995**, *113*, 131−134.
(31) Saalwächter, K.; Graf, R.; Demco, D. E.; Spiess, H. W. *J. Magn. Reson.* **1999**, *139*, 287−301.
(32) Saalwächter, K.; Spiess, H. W. *J. Chem. Phys.* **2001**, *114*, 5707−5728.
(33) Emshviller, M.; Hahn, E. L.; Kaplan, D. *Phys. Rev.* **1960**, *118*, 414−424.
(34) Wang, P.-K.; Slichter, C. P.; Sinfelt, J. H. *Phys. Rev. Lett.* **1984**, *53*, 82−85.
(35) Gullion, T.; Schaefer, J. *J. Magn. Reson.* **1989**, *81*, 196−200.
(36) Gullion, T. *Concepts Magn. Reson.* **1998**, *10* (5), 277−289.
(37) Pan, Y.; Gullion, T.; Schaefer, J. *J. Magn. Reson.* **1990**, *90*, 330−340.
(38) Fyfe, C. A.; Lewis, A. R.; Chezeau, J.-M. *Can. J. Chem.* **1999**, *77*, 1984−1993.
(39) Gullion, T.; Pennington, C. *Chem. Phys. Lett.* **1998**, *290*, 88−93.
(40) Garbow, J. R.; Gullion, T. *J. Magn. Reson.* **1991**, *91* (2), 442−445.
(41) Cohen-Addad, J. P. *Prog. Nucl. Magn. Reson. Spectrosc.* **1993**, *25*, 1−316.
(42) Sotta, P.; Deloche, B. *Macromol.* **1990**, *23*, 1999−2007.
(43) Bak, M.; Rasmussen, J. T.; Nielsen, N. C. *J. Magn. Reson.* **2000**, *147*, 296−330.
(44) Wolfram, S. *Mathematica. A System for Doing Mathematics by Computer*; Addison-Wesley Publishing Company: Reading, MA, 1991.
(45) Bertmer, M.; Gasper, L.; Demco, D. E.; Blümich, B.; Litvinov, V. M. *Macromol. Chem. Phys.* **2004**, *205*, 83−94.
(46) Hong, M.; Schmidt-Rohr, K.; Pines, A. *J. Am. Chem. Soc.* **1995**, *117*, 3310−3311.
(47) Schnell, I.; Spiess, H. W. *J. Magn. Reson.* **2001**, *151*, 153−227.
(48) Reif, B.; Jaroniec, C. P.; Rienstra, C. M.; Hohwy, M.; Griffin, R. G. *J. Magn. Reson.* **2001**, *151*, 320−327.
(49) Graf, R.; Demco, D. E.; Hafner, S.; Spiess, H. W. *Solid State Nucl. Magn. Reson.* **1998**, *12*, 139−152.
(50) Mueller, K. T.; Jarvie, T. P.; Aurentz, D. J.; Roberts, B. W. *Chem. Phys. Lett.* **1995**, *242*, 535−42.
(51) Bertmer, M.; Eckert, H. *Solid State Nucl. Magn. Reson.* **1999**, *15*, 139−52.
(52) Kentgens, A. P. M.; Veeman, W. S.; van Bree, J. *Macromolecules* **1987**, *20*, 1234−1237.
(53) Schaefer, J. *Macromolecules* **1972**, *5*, 427−440.